PIBB 生物化学与生物物理进展
Progress in Biochemistry and Biophysics
2010, 37(10): 1108~1119
www.pibb.ac.cn

The Alterations of Energy Metabolism-related Protein Patterns in Brown Adipose Tissue of Rats During Cold-induced Thermogenesis

YANG Yue[1,2], GONG Wei[1,2], WANG Wei-Wei[1,2], YU Xiao-Min[1], HU Song-Nian[1], YU Jun[1]*
([1] *CAS Key Laboratory of Genome Sciences and Information, Beijing Institute of Genomics, The Chinese Academy of Sciences, Beijing* 100029, China;
[2] *Graduate University of The Chinese Academy of Sciences, Beijing* 100049, China)

Abstract The physiological role of brown adipose tissue (BAT) is quite different from that of white adipose tissue (WAT) by dissipating energy as heat instead of generating ATP. Mitochondrion is an essential organelle that plays a crucial role in energy production and cellular homeostasis. To gain a better understanding of energy metabolism in BAT, mitochondria were isolated and a systematic analysis of protein patterns was performed in WAT and BAT of rat with two-dimensional gel electrophoresis. Differentially expressed proteins were identified using mass spectrometry and it was found that the proteins involved in lipid and amino acid metabolisms, TCA cycle, and respiratory chain are more abundant in BAT than in WAT, which are further up-regulated in response to cold exposure in BAT. Furthermore, the study reveals, for the first time, a subset of COQ genes required for Coenzyme Q biosynthesis are significantly up-regulated after cold exposure in BAT. These findings suggest that Coenzyme Q increase is implicated in the non-shivering thermogenesis and contribute new data for understanding the unique process of energy metabolism in BAT.

Key words brown adipose tissue, cold acclimation, thermogenesis, coenzyme Q
DOI: 10.3724/SP.J.1206.2010.00231

White adipose tissue (WAT) and brown adipose tissue (BAT) perform very different functions in mammals since WAT stores energy from metabolic fuels as fat while BAT dissipates energy as heat [1–3]. BAT is responsible for a major portion of thermogenesis in newborn rodents exposed to cold and in hibernators during arousal [4–6]. The development of BAT gives small mammals evolutionary advantage to maintain constant body temperature. BAT is also important in mediating diet-induced thermogenesis [7–8] and thought to function in protecting against obesity by reducing fat storage[9–12]. Mitochondria are fundamental sites of mediating effects on energy dissipating. BAT can be distinguished from WAT by comprising a large number of mitochondria packed with well developed cristae. A study of isolated mitochondria revealed an elevated respiratory rate in brown fat[13]. In addition, it was demonstrated a particular mechanism operated in these mitochondria that the respiration was loosely coupled to ADP phosphorylation [14]. Thus, not only increased mitochondrial biogenesis but also the uncoupling of electron transport from ATP synthesis leads to heat producing in BAT.

One firmly established site of uncoupling is the leakage of protons back across the mitochondria inner membrane bypassing ATP synthase and converting energy stored within the protonmotive force directly to heat[15]. It is catalyzed by uncoupling protein-1(UCP-1), a carrier protein uniquely expressed in the mitochondrial inner membrane of brown adipocytes [16–17]. Indeed, gene-knockout mice lacking UCP-1 have decreased body temperature during cold exposure[18]. Apart from the well known increase in UCP-1 content, changes in mitochondrial proteins involved in the respiratory chain, FFA uptake, and β-oxidation, as well as in the TCA cycle, are observed.

It is possible that other enzymes or proteins work together with UCP-1 for efficient energy dissipation in

*Corresponding author.
Tel: 86-10-82995357, E-mail: junyu@big.ac.cn
Received: April 28, 2010 Accepted: June 10, 2010

BAT. Coenzyme Q (ubiquinone, CoQ) plays an essential role in the mitochondrial respiratory chain of all animal and plant cells [19]. It has been established CoQ behaves as a mobile homogeneous pool which carries electrons between flavoproteins (Complex Ⅰ and Ⅱ and other dehydrogenases) and the bc1 complex (Complex Ⅲ) in the inner mitochondrial membrane[19]. In addition, CoQ functions as a cofactor for uncoupling proteins and other mitochondrial dehydrogenases [20]. Previous studies showed that CoQ pool function in glycerol-3-phosphate oxidation in brown adipose tissue mitochondria [21]. This flavin-dependent dehydrogenase is localized on the outer surface of the inner mitochondrial membrane, catalyzes the transfer of hydrogen from glycerol-3-phosphate to ubiquinone, thus forming one of the most important branches of the mitochondrial respiratory chain. The highest activity of this enzyme was found in insect flight muscle and in brown adipose tissue of newborn or cold-adapted adult mammals[22]. It has been evidenced that transgenic mice overexpressing glycerol-3-phosphate dehydrogenase are lean and have increased thermogenesis [23]. Factors regulating CoQ biosynthesis remain unclear. There are at least ten genes (COQ genes) involved in a complex biosynthetic pathway [24]. Products of eight genes have been described to participate in CoQ biosynthesis in bacteria, yeasts, and nematodes [25-26]. Different human genes homologous to those described in yeast are thought to participate in CoQ biosynthesis. The known genes involved in the CoQ biosynthesis pathway are highly conserved. In particular, clk-1/coq7 homologous are highly conserved among eukaryotic organisms [27].

Here we apply the high resolution 2-DE and mass spectrometry analysis to identify the genes for which their expression levels are specifically regulated in BAT. We found that cold induced up-regulation of COQ7, COQ8, and COQ9, which are considered to have both a regulatory and kinetic role in CoQ biosynthesis. Our findings suggest that an increase in CoQ levels is implicated in the unique process of energy metabolism in brown fat and may contribute to protecting against cold by heat producing.

1 Materials and methods

1.1 Animals

Sprague-Dawley rats (200 g) were kept in a controlled environment ((20±2)℃, 12 h/12 h light/dark photoperiod) and fed a standard chow diet with water *ad libitum*. Animals were divided into two groups of 10 rats each. One group was kept in a climate chamber at 4℃ for 24 days; the control group was kept at room temperature.

1.2 Materials and antibodies

The following antibodies were used for Western blotting: anti-UCP-1 antibody (Sigma-Aldrich, MO, USA) was used in a dilution of 1∶1 000; anti-aldehyde dehydrogenase 1(ALDH1) antibody (Thermo scientific, IL, USA) was used in a dilution of 1∶1 000; anti-ATP synthase β subunit antibody (BD Bioscience, CA, USA) was used in a dilution of 1∶10 000; anti-glyceraldehyde-3-phosphate dehydrogenase (GAPDH) antibody (Millipore, MA, USA) was used in a dilution of 1∶100; anti-aldehyde reductase (ALR) antibody (Santa Cruz, CA, USA) was used in a dilution of 1∶500. Immobiline pH gradient strips and ampholytes were purchased from Amersham Biosciences. Nycodenz was purchased from Axis-Shield (Oslo, Norway). All other biochemicals were obtained from Sigma or Bio-Rad unless otherwise stated. Adult male Sprague-Dawley rats were purchased from Laboratory Animal Center of Chinese Academy of Medical Sciences (CAMS).

1.3 Isolation of rat adipose tissue mitochondria

Mitochondria were isolated according to the procedure of Barbara Cannon[28] with some modifications as outlined below. Briefly, animals were sacrificed and both adipose tissues were promptly removed and placed in ice-cold homogenization buffer consisting of 50 mmol/L sucrose, 200 mmol/L mannitol, 1 mmol/L EDTA, 0.5 mmol/L EGTA, and a mixture of protease inhibitor (1 mmol/L phenylmethylsulfonylfluoride, PMSF) and phosphatase inhibitors(0.2 mmol/L Na_3VO_4, 1 mmol/L NaF). After mincing with scissors and washing to remove blood, the tissue samples were homogenized in a glass Dounce homogenizer at the ratio of 5 ml of the homogenization buffer per gram of the tissue. The homogenate was filtered through two layers of gauze and centrifuged twice at 1 000 *g* for 10 min at 4℃ to remove nuclei and unbroken cells. Mitochondria were isolated by centrifugation of the supernatant at 8 500 *g* for 20 min at 4℃. The pellets were washed twice with homogenization buffer and suspended in 12 ml of 25% Nycodenz, then layered on the following discontinuous Nycodenz gradients: 5 ml of 34% and 8 ml of 30%, and this was topped off with 8 ml of 23% and finally 3 ml of 20% and were

centrifuged for 90 min at 52 000 *g* at 4℃. The mitochondria were observed as a tight yellow-brown band at the 25% ~ 30% interface. The band was collected and diluted with the same volume homogenization buffer and then centrifuged at 15 000 *g* for 15 min at 4℃. The functional integrity of the purified mitochondrial was measured by assaying of marker proteins from mitochondria and cytosol with Western blotting. Their structural integrity was assessed by transmission electron microscopy.

1.4 Mitochondrial morphology and function assay

The mitochondrial pellet was fixed with 2% glutaradlehyde plus 2% tannic acid in 0.1 mol/L cacodylate (pH 7.4) for 1 h at room temperature, followed by 1.0% OsO_4 plus 1.0% potassium ferrocyanide for 1 h at 4℃. The sections were post stained with uranyl acetate and lead citrate and observed with a JEOL-2010 microscope. For Western blotting, equal amount of mitochondrial and cytosolic proteins were loaded in each lane of a 10% SDS-PAGE gel. After gel electrophoresis and protein transfer, the membranes were probed with various primary and corresponding secondary antibodies against marker proteins from mitochondrial and cytosolic compartments. Immunoreactivity was detected with an ECL system (Amersham Biosciences).

1.5 Two-dimensional gel electrophoresis and image analysis

For IEF, 150 μg of proteins were diluted to a final volume of 350 μl in a rehydration solution containing 7 mol/L urea, 2 mol/L thiourea, 4% (*w*/*v*) CHAPS, 55 mmol/L DTT, and 0.5%(*v*/*v*) IPG buffer(pH 3 ~ 10, linear), and then were introduced into 18 cm, pH 3 ~ 10, linear IPG strips. The IPG strips were rehydrated and focused at 20℃, starting with passive rehydration for 4 h followed by 8 h active rehydration at 50 V. The focusing was started at 250 V for 15 min (rapid voltage ramping), 500 V for 1 h, and 1 000 V for 1 h followed by linearly ramping to 8 000 V and then kept at 8 000 V until 60 000 V·h were reached. Isoelectric focusing was carried out on an Ettan IPGphor system (Amersham Biosciences). Following IEF, proteins were reduced by equilibrating the stripes for 20 min in a solution containing 50 mmol/L Tris-HCl (pH 8.8), 6 mol/L urea, 30% glycerol, 2% SDS, 1% (*w*/*v*) DTT and then alkylated by equilibration for 20 min in a similar solution with DTT replaced by 2.5% (*w*/*v*) iodoacetamide. IPG strips were then embedded in low melting agarose onto the top of 12% polyacrylamide gel. SDS-PAGE was performed using Ettan DALT Ⅱ (Amersham Biosciences) with a programmable power control and protein spots were visualized by silver staining. At least triplicate gels were performed for each sample.

The gels were acquired with an image scanner in transmission mode and saved as TIFF files. Image analysis was accomplished using ImageMaster 2D Platinum software(version 5.0, Amersham Biosciences) on a set of three gels per sample for spot detection, quantification, matching and comparative analysis. The volumes of protein spots, which were normalized against the total volume of all the spots in the gel, were compared between different groups. This normalized spot volume takes into account variations due to protein loading and staining by considering the total volume over all the spots present in the gel. Spots with a volume variation ratio greater than 2 were considered differential. The corresponding *P*-values were determined by using the independent Student's *t*-test. Analyzed protein spots with a *P*-value < 0.05 were considered to be statistically significant and were subsequently treated for identification by mass spectrometry.

1.6 MS-based protein identification

Protein spots were excised from silver-stained gels, washed 3 times with ultrapure water, dehydrated with 100% acetonitrile, reduced with 10 mmol/L DTT in 100 mmol/L NH_4HCO_3 at 56℃ for 1 h, alkylated with 55 mmol/L iodoacetamide in 100 mmol/L NH_4HCO_3 in the dark for 45 min followed by a process of washing and drying. The protein particles were digested overnight at 37℃ with 10 μl 25 mmol/L NH_4HCO_3 containing 0.05 g/L trypsin. Finally, 1% TFA was added to stop the enzymatic reaction, and the resultant peptides were subjected to mass spectrometry.

Peptides were cocrystallized with a matrix solution of 4 g/L α-cyano-4-hydroxycinamic acid (Sigma) in 70% acetonitrile and 0.1% TFA on MALDI target plates for MS analysis using an ultraflex Ⅲ TOF/TOF system (Bruker Daltonics, MA, USA). Peptide mass spectra were acquired in reflectron mode with 100 shots accumulated per spectrum in MS mode and 400 shots accumulated per spectrum in MS/MS mode. Internal calibration was performed using autodigestion peaks of trypsin. The spectra were processed using FlexAnalysis 2.2 and BioTools 3.0 software tools. The MS together with MS/MS spectra

were searched using MASCOT version 1.9 (Matrix Science) against National Center for Biotechnology Information non-redundant (NCBInr) (2 524 882 sequences) and Swiss-Prot databases (16 677 entries). Searches were performed with taxonomy of rattus norvegicus, fixed modification of carbamidomethylation of cysteines and variable modification of acetyl-N terminus, oxidation-M (methionine), pyro-N terminus. One trypsin miscleavage was allowed. Peptide mass tolerance and fragment mass tolerance were set to < 100 ppm and < 0.7 u, respectively. High confidence identifications have statistically significant search scores (greater than 95% confidence interval, equivalent to MASCOT expect value < 0.05), are consistent with the protein experimental p*I* and M_r and account for the majority of ions present in the mass spectra.

1.7 Quantitative real-time PCR

Quantitative real-time PCR analysis (qRT-PCR) was performed using ABI PRISM 7300 system (Foster City, CA, USA) and monitored with SYBR Green as described previously [29] . Total RNAs were extracted with Trizol (Invitrogen) and removed DNA contaminations with RNase-free DNase Ⅰ. Primer pairs used in the experiments are as follows: COQ7 (forward, 5′ CATCACTACAACAACCAGATCCGC 3′, reverse, 5′ TCCGGCCTGGATAAGTCTCTTCAA 3′); COQ8 (forward, 5′ TGCCAAGAAGAGTCTGCGTTCTGA 3′, reverse, 5′ AAAGATCTTGGCCAGGTGAGGGTT 3′); COQ9 (forward, 5′ CACAACCAAGGTCCAAAGGCAACA 3′, reverse, 5′ GCAATGCACACTGGTGTCTGTGAT 3′). GAPDH expression assay with the forward primer 5′ ATGTGTCCGTCGTGGATCTGAC 3′ and reverse primer 5′ AGACAACCTGGTCCTCAGTGTAG 3′ was used as endogenous control.

1.8 Statistics

Data duplicates are presented as $\bar{x} \pm s$. Significant differences between data sets were assessed with Student's *t*-test. Differences were considered significant at $P < 0.05$.

2 Results

2.1 Morphology of adipose tissues and characterization of the isolated mitochondria

To avoid cross-contamination, we obtained BAT from the inter-scapular of rats, whereas we isolated WAT around internal organs including kidney and testis, which contain no BAT. WAT and BAT of rat were fixed, sectioned, stained, and examined microscopically. As shown in Figure 1a, stained tissue sections at low magnification exhibited dramatic structural differences between the two tissues. White adipocytes (Figure 1a, upper panel) have a scant ring of cytoplasm surrounding a single large lipid droplet. Their nuclei are flattened and eccentric within the cell. Brown adipocytes (Figure 1a, lower panel) are polygonal in shape and have a considerable volume of cytoplasm and contain multiple lipid droplets of varying sizes. Their nuclei are round and almost centered in the cells.

The procedure used to purify mitochondria from WAT and BAT involved three differential centrifugations followed by Nycodenz density gradient centrifugation. The structural integrity of the purified mitochondria was confirmed by electron microscopy where the mitochondria are typically round with cristae across their entire width and most of the structures are intact (Figure 1b).

The purity of mitochondria was assessed by Western blotting of marker proteins from mitochondria including ATP synthase and ALDH and cytosolic marker protein including ALR and GAPDH. ATP synthase and ALDH were specifically detected in the purified mitochondria fraction, the intensity was much greater than in the initial homogenate, and this fraction

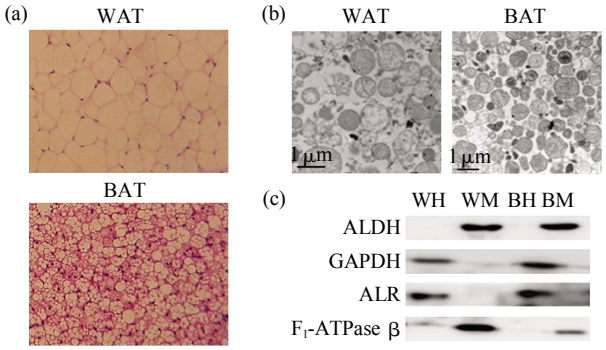

Fig. 1 Morphology of adipose tissue and characterization of the isolated mitochondria

(a) Hematoxylin and Eosin (HE) stains of two adipose tissues. Examination of sections of white adipose tissue (upper panel) and brown adipose tissue (lower panel) reveal dramatic differences in structure. Magnification, 20×10. (b) Morphology of purified mitochondria of white adipose tissue (left panel) and brown adipose tissue (right panel). The bar represents 1.0 μm. (c) Western blotting of equal amounts of mitochondrial proteins (15 μg) with indicated antibodies against marker proteins from mitochondria and cytosol. WH, cytosolic fraction of white adipose tissue; WM, mitochondrial fraction of white adipose tissue; BH, cytosolic fraction of control brown adipose tissue; BM, mitochondrial fraction of control brown adipose tissue.

lacked contamination of cytosolic proteins such as ALR and GAPDH (Figure 1c).

2.2 2-DE gel analysis of mitochondrial proteins in adipose tissue and mitochondrial remodeling in response to cold exposure in BAT

To elucidate the processes of energy metabolism of WAT and BAT, we carried out 2-DE analysis of the mitochondrial proteins. This powerful technique allowed us to separate and detect protein spots distributed over the 3～10 pH gradients in this study. For each sample, at least triplicate gels were performed, and more than 90% of overlapped rates of 2-DE spots were achieved in these parallel gels for each sample which indicated that parallel 2-DE images were reproducible and acceptable for differential analysis of 2-DE spots. Silver-stained gels of mitochondrial proteins from rat WAT and BAT are well-resolved as depicted in Figure 2. Most 2-DE spots in the two samples were found in high p*I* region. This observation means that basic proteins dominate the mitochondria proteome of both adipose tissues. Of approximately 470 spots analyzed in the molecular mass range of 14～96 ku, quantitative image analysis revealed a total of 50 protein spots that changed their intensities significantly ($P < 0.05$) by 2-fold or greater when comparing spots from mitochondria of rat WAT with those from BAT. All the up and down-regulated protein spots are shown. Based on 2-DE analysis, we found 6 and 44 protein spots detected in mitochondrial preparations showing down-regulated (Figure 2a) and up-regulated trends (Figure 2b) between WAT and BAT, respectively.

To study the effects of cold exposure on mitochondrial protein expression level, we used 2-DE analysis to display and compare mitochondrial proteins of BAT from cold-adapted and control animals. Of approximately 500 spots analyzed in the molecular mass range of 14～96 ku, quantitative image analysis revealed a total of 21 protein spots that changed their intensities significantly ($P < 0.05$) by 2-fold or greater between control and cold-adapted animals. Spots modulated by cold treatment are indicated with an

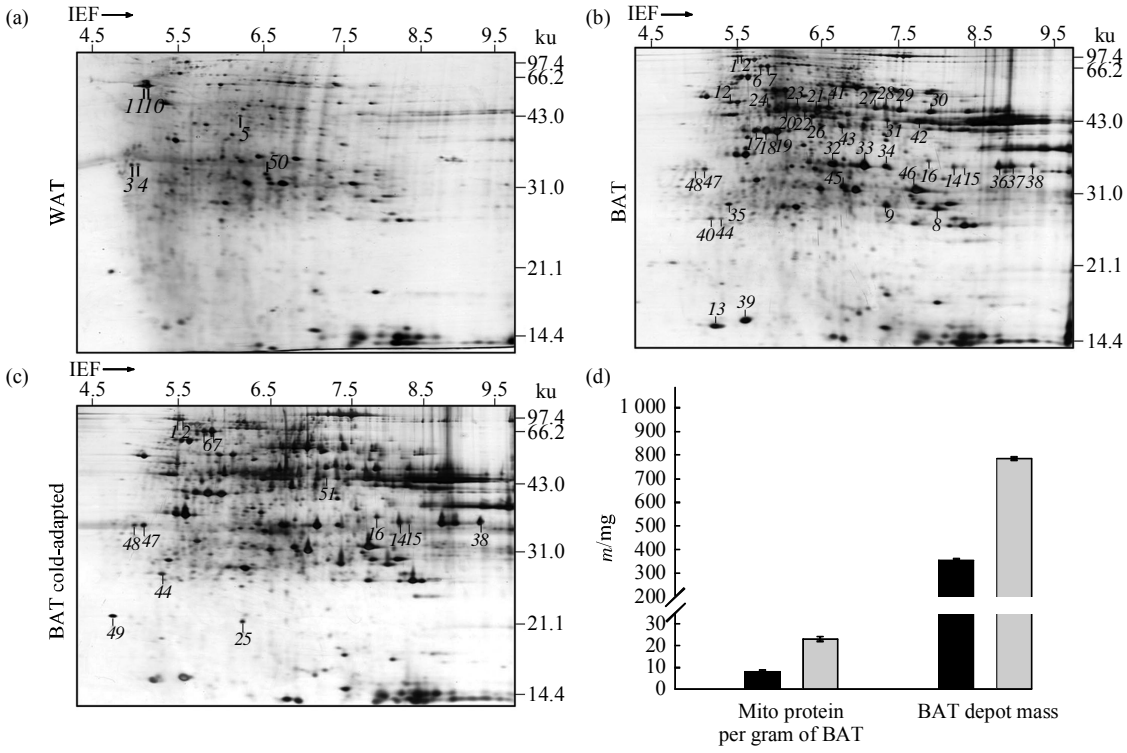

Fig. 2 Representative 2-DE gels of mitochondrial proteins of adipose tissue

(a) Quantitative image analysis revealed a total of 6 protein spots that were down-regulated significantly ($P < 0.05$) in brown fat mitochondria comparing with white fat mitochondria. The differential spots are numbered. (b) Quantitative image analysis revealed a total of 44 protein spots that were up-regulated significantly ($P < 0.05$) in brown fat mitochondria comparing with white fat mitochondria. The differential spots are numbered. (c) A total of 14 protein spots that changed their intensities significantly ($P < 0.05$) by more than 2-fold upon cold exposure in brown fat mitochondria. The names of the proteins differentially expressed are shown in Table 1. (d) Wet weight of brown adipose tissue (mg); values are $\bar{x} \pm s$ (n=5). Mitochondrial protein amounts in the per gram of BAT (expressed in mg) were determined. ■: Control; □: Cold.

arrow (Figure 2c). All the protein spots were up-regulated. To further functionally characterize the BAT mitochondrial proteome, we investigate its remodeling in response to cold exposure. Brown fat depots were isolated and the mitochondrial fractions were extracted after 24-days cold exposure. Both BAT depot mass and extracted mitochondrial proteins increased significantly. The brown adipocyte recruitment led to about 2.2-fold of the BAT mass per animal and the mass of mitochondria per gram of BAT was also increased at least 2.7-fold (Figure 2d). These results are in perfect agreement with previous studies [30–31].

2.3 Identification of the differentially expressed proteins

The differentially expressed proteins were excised from the 2-DE gels, in-gel digested by trypsin, and analyzed by a MALDI-TOF/TOF mass spectrometer. In total, 49 differentially expressed proteins between WAT and BAT were identified either by PMF or MS/MS analysis. Spot identities, accession numbers, MOWSE (molecular mass search) scores, percent coverage, p*I*, molecular mass are presented (Table 1). Some spots are predicted to be the same protein. This could be possible *via* different post-translational modification. The results of spot 10 are shown as an example (Figure 3a). The identified proteins are categorized into four different functional groups according to gene ontology (GO), including lipid and amino acid metabolism, TCA cycle, oxidative phosphorylation, signaling and protein synthesis. The largest functional category was proteins involved in oxidative phosphorylation (30.6%). This group corresponded to 15 differential protein spots between WAT and BAT, 14 of which were up-regulated in BAT, however, the expression level of F_1-ATPase β subunit was much lower in BAT for more than 2-fold. In addition, the expression level of proteins involved in metabolisms of lipid (such as HCDH, MCDH and ETF) and amino acid (such as HMG-CoA lyase, ICDH and BCKD) were more abundant in BAT, which strongly augment the substrate availability and evidence a greater activity of TCA cycle. We found that four enzymes involved in TCA cycle were up-regulated in BAT: aconitate hydratase, 2.2-fold; pyruvate dehydrogenase, 2.1-fold; fumarate hydratase, 2.5-fold; and isocitrate dehydrogenase, 3.2-fold. A total of 20 differentially expressed proteins in response to cold exposure were successfully identified by MS analysis. In our comparative proteomic analysis, we found that UCP-1 is strongly up-regulated by cold adaptation (3.6-fold for the same amount of mitochondrial proteins). In addition, we found that cold induced up-regulation of COQ7 (spot 25), COQ8 (spot 49) and COQ9 (spots 47 and 48), which are considered to have a regulatory role in CoQ biosynthesis and thus function in efficient energy dissipation in BAT.

Table 1 Differentially expressed mitochondrial proteins in WAT, control and cold-adapted BAT identified by MS

SN[1]	NCBI accession No.	Protein	T (ku/p*I*)[2]	O (ku/p*I*)[3]	Score	MP[4]	C/%[5]	Type[6]
Lipid metabolism								
14	7387725	Short chain L-3-hydroxyacyl-CoA dehydrogenase	32.9/8.33	32.5/8.25	144	13	39	BC>B>W
15	7387725	Short chain L-3-hydroxyacyl-CoA dehydrogenase	32.9/8.33	32.5/8.35	126	12	38	BC>B>W
36[7]	7387725	Short chain L-3-hydroxyacyl-CoA dehydrogenase	32.9/8.33	32.6/8.85	105	9	25	BC≈B>W
37[7]	7387725	Short chain L-3-hydroxyacyl-CoA dehydrogenase	32.9/8.33	32.5/8.95	121	10	35	BC≈B>W
31	113018	Acetyl-coenzyme A dehydrogenase, medium chain	43.7/7.68	42.1/7.41	102	13	22	BC≈B>W
32	57527204	Electron transfer flavoprotein alpha polypeptide	32.9/6.90	32.5/6.80	132	14	50	BC≈B>W
33	57527204	Electron transfer flavoprotein alpha polypeptide	32.9/6.90	32.5/7.20	187	19	57	BC≈B>W
34	57527204	Electron transfer flavoprotein alpha polypeptide	32.9/6.90	34.5/7.38	129	14	46	BC≈B>W
42	113018	Acetyl-coenzyme A dehydrogenase, medium chain	43.7/7.68	42.1/7.82	168	18	31	BC≈B>W
43	1168286	Acetyl-coenzyme A dehydrogenase, short chain	42.2/6.38	41.8/6.80	110	16	27	BC≈B>W
45	51948412	Electron transfer flavoprotein beta polypeptide	27.6/7.81	27.6/6.95	110	10	43	BC≈B>W
46	51948412	Electron transfer flavoprotein beta polypeptide	27.6/7.81	27.5/7.80	146	14	52	BC≈B>W
51	18426866	Acetyl-CoA acyltransferase 2	32.9/8.33	32.6/8.85	191	16	43	BC>B≈W

Continued

SN[1]	NCBI accession No.	Protein	T (ku/p*I*)[2]	O (ku/p*I*)[3]	Score	MP[4]	C(%)[5]	Type[6]
Amino acid metabolism								
16	2495261	Hydroxymethylglutaryl-CoA lyase	31.4/7.50	33.2/7.90	82	8	18	BC>B>W
24[7]	129032	Branched-chain keto acid decarboxylase subunit alpha	45.6/5.93	45.5/5.85	104	15	36	BC≈B>W
26	6981112	Isovaleryl-coenzyme A dehydrogenase	43.1/6.12	42.5/6.40	123	17	39	BC≈B>W
TCA cycle								
6	78174343	Pyruvate dehydrogenase E2 component	58.7/5.70	66.1/5.70	203	21	40	BC>B>W
7	78174343	Pyruvate dehydrogenase E2 component	58.7/5.70	66.1/5.80	144	17	35	BC>B>W
20	129064	Pyruvate dehydrogenase E1 component alpha subunit	40.2/6.82	43.5/6.15	87	12	24	BC≈B>W
21[7]	129064	Pyruvate dehydrogenase E1 component alpha subunit	40.2/6.82	43.0/6.45	197	20	37	BC≈B>W
22	129064	Pyruvate dehydrogenase E1 component alpha subunit	40.2/6.82	43.5/6.35	86	12	24	BC≈B>W
23	129064	Pyruvate dehydrogenase E1 component alpha subunit	40.2/6.82	43.5/6.25	175	20	37	BC≈B>W
17	16758446	Isocitrate dehydrogenase 3 [NAD] subunit alpha	36.7/5.72	36.5/5.65	99	11	35	BC≈B>W
18	16758446	Isocitrate dehydrogenase 3 [NAD] subunit alpha	36.7/5.72	36.5/5.83	119	11	32	BC≈B>W
19[7]	16758446	Isocitrate dehydrogenase 3 [NAD] subunit alpha	36.7/5.72	36.5/5.95	152	16	41	BC≈B>W
27	120605	Fumarate hydratase	50.0/8.27	49.4/7.25	106	15	35	BC≈B>W
28	40538860	Aconitate hydratase	82.5/7.15	50.5/7.31	94	18	21	BC≈B>W
29[7]	120605	Fumarate hydratase	50.0/8.27	49.4/7.55	117	15	35	BC≈B>W
30	120605	Fumarate hydratase	50.0/8.27	49.4/8.05	80	9	27	BC≈B>W
Oxidative phosphorylation								
1	53850628	NADH-ubiquinone oxidoreductase 75ku subunit	76.9/5.28	76.5/5.45	107	12	21	BC>B>W
2	53850628	NADH-ubiquinone oxidoreductase 75ku subunit	76.9/5.28	76.5/5.50	125	18	33	BC>B>W
35	51092268	NADH-ubiquinone dehydrogenase flavoprotein 2	23.9/5.07	25.1/5.30	87	11	39	BC≈B>W
8	52001457	Ubiquinol-cytochrome c reductase iron-sulfur subunit	21.5/7.67	25.5/8.05	114	11	31	BC≈B>W
9	52001457	Ubiquinol-cytochrome c reductase iron-sulfur subunit	21.5/7.67	25.6/7.31	62	7	22	BC≈B>W
12	51948476	Ubiquinol-cytochrome c reductase core protein Ⅰ	49.4/5.22	49.5/5.30	226	21	44	BC≈B>W
40[7]	27661165	NADH-ubiquinone dehydrogenase, Fe-S protein 8	24.0/5.89	24.1/5.15	60	5	26	BC≈B>W
44[7]	27661165	NADH-ubiquinone dehydrogenase, Fe-S protein 8	24.0/5.89	24.1/5.25	138	14	39	BC>B>W
13	24233541	Cytochrome c oxidase subunit Va	12.4/5.01	14.1/5.20	63	7	44	BC≈B>W
39	16758362	Cytochrome c oxidase subunit Vb	10.8/5.22	14.2/5.50	64	9	42	BC≈B>W
3[7]	203033	F_1-ATPase beta subunit(fragment)	37.2/4.97	30.2/4.90	140	17	46	BC≈B<W
4	203033	F_1-ATPase beta subunit(fragment)	37.2/4.97	30.2/4.95	71	8	33	BC≈B<W
10[7]	54792127	F_1-ATPase beta subunit	51.7/4.95	51.5/5.05	286	36	40	BC≈B<W
11[7]	54792127	F_1-ATPase beta subunit	51.7/4.95	51.5/4.95	157	14	28	BC≈B<W
38	136690	Uncoupling protein 1	33.1/9.21	32.5/9.15	95	8	21	BC>B>W
47	51259441	COQ9_ubiquinone biosynthesis protein	30.2/4.87	30.5/4.95	120	15	41	BC>B>W
48	51259441	COQ9_ubiquinone biosynthesis protein	30.2/4.87	30.5/4.90	101	12	39	BC>B>W
49[7]	61557218	COQ8_ubiquinone biosynthesis protein	22.0/4.88	22.1/4.62	94	8	18	BC>B≈W
25	2851472	COQ7_ubiquinone biosynthesis protein	20.1/5.64	21.5/6.20	63	4	18	BC>B>W
Signaling								
5	6978501	Annexin A1	38.7/7.13	36.5/6.35	76	7	26	BC≈B<W
Protein synthesis								
41	62641274	Tu-translation elongation factor	50.1/9.10	50.3/6.71	182	20	39	BC≈B<W
Unknown protein								
50	–	–	–	27.4/7.80	–	–	–	BC≈B<W

[1] Spot number corresponding to spots in Figure 2. [2] Theoretical molecular mass (ku) and p*I* of the matched proteins, derived from ExPASy web site (expasy.org/) according to the mature protein calculated with Compute p*I*/*M*. [3] Observed molecular mass (ku) and p*I* were measured from two-dimensional gels. [4] Number of mass values matched. [5] The percent ratio of all amino acids from matched peptide to the total number of amino acids in the protein. [6] Protein expression patterns BC=cold-adapted BAT, B=control BAT, and W=WAT; "≈" stands for a difference within 2 fold between each two sample. [7] Proteins identified and confirmed by MALDI TOF/TOF.

To confirm the results obtained in 2D gels, Western blot analysis was carried out for prominent proteins. UCP-1 and F_1-ATPase β subunit were selected, and their expression in WAT and BAT was examined. UCP-1 was detected with a high intensity of immuoreactivity in mitochondria of BAT while it was not detected in WAT, whereas F_1-ATPase β subunit displayed attenuated intensities of immuoreactivity in BAT (Figure 3b and 3c). These results were considerably consistent with the proteomic observations.

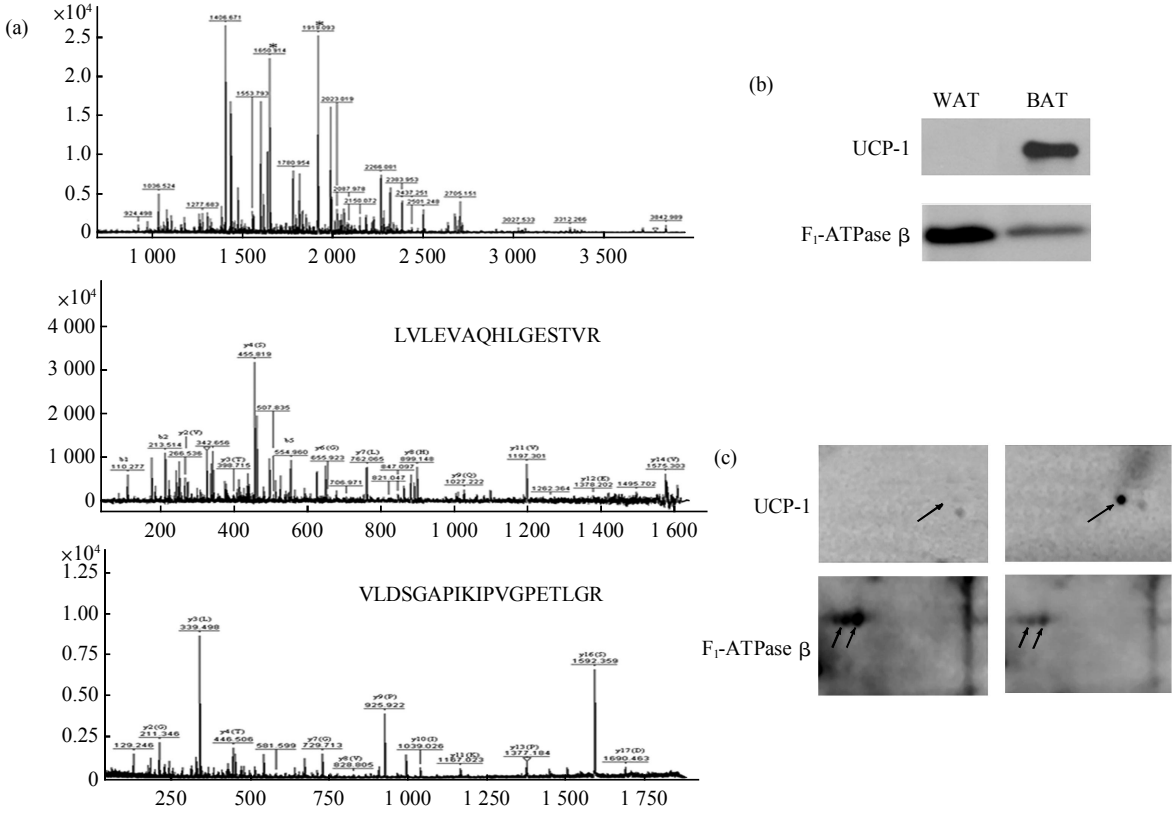

Fig. 3 Identification of differentially expressed proteins

(a) Identification of F_1-ATPase β subunit based on results from MALDI-TOF MS (upper panel). The MALDI-TOF/TOF spectra of parent ions of 1 650.91 (middle panel) and 1 919.09 (lower panel) are showed as examples of data quality. (b) Expression analysis by Western blot. The mitochondrial protein extracts from white and brown adipose tissue of rat representing equal amounts of protein (20 μg) were run on 12% SDS gels and transferred to PVDF membranes. The membranes were probed with anti-UCP-1 antibody and anti-ATPase (β) antibody. The immunoreactive bands are shown. (c) The identification by mass spectrum was further confirmed with 2D-Western blot. The mitochondrial proteins from white and brown adipose tissue were transferred from 2D PAGE gels to PVDF membranes. The membrane was probed with anti-UCP-1 antibody and anti-ATPase (β) antibody. The additional UCP-1 spot in BAT that is missing in white fat and the differential ATPase (β) spots between two tissues are indicated with arrows.

2.4 Specific assessment of COQ gene regulation in response to cold exposure

The typical regions were enlarged in Figure 4a to show comparisons of mitochondrial COQ between control and cold-adapted brown fat. The protein spot comparison and their correlation with relative expression levels shown as normalized volume are given in Figure 4b. The expression of COQ7, COQ8, and COQ9 were highly up-regulated after cold exposure in brown adipose tissue. Real-time PCR confirmed up-regulation of COQ mRNA by cold exposure (Figure 4c). Collectively, these results suggest that effects on the expression of COQ may contribute, at least partially, to cold-induced heat producing through regulating energy dissipation in brown adipose tissue.

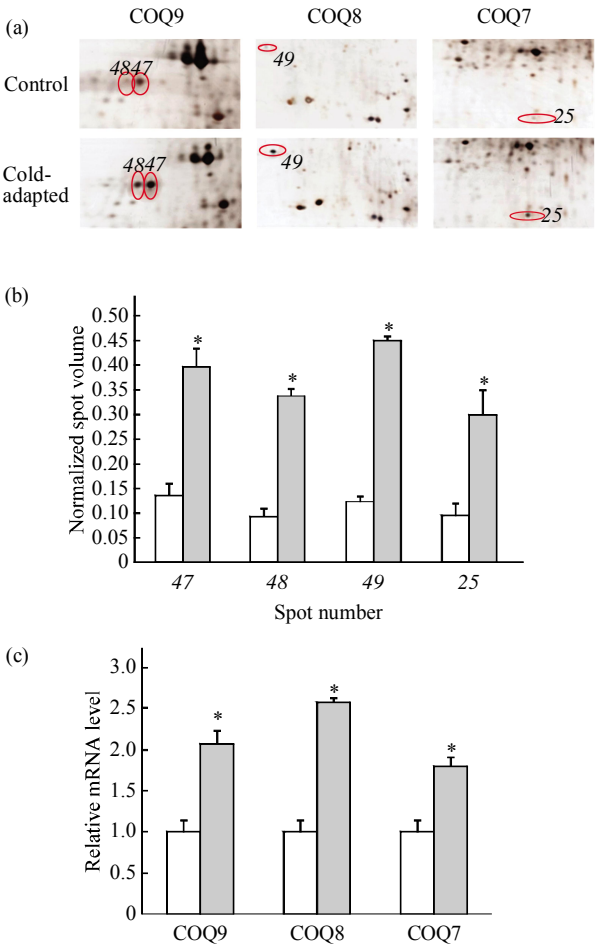

Fig. 4 Specific assessment of COQ gene regulation in response to cold exposure

(a) Close-up of the region of the gels showing up regulation significantly (*t*-test, $P < 0.05$) of CoQ biosynthesis protein including COQ9, COQ8 and COQ7 (red circle) upon cold exposure in brown fat. (b) The degree of differential expression in the two samples is shown in the histogram below the corresponding gel part. The expression quantification is presented as a grouped bar chart with error bars. Each bar represents average spot abundance expressed as normalized volume ± S.D. The vertical axis shows spot normalized volume. The expression of COQ9, COQ8 and COQ7 are highly up-regulated upon cold exposure (*$P < 0.01$, student's *t*-test). (c) Results of real-time PCR performed on cDNA from rat brown adipose tissue after cold exposure. Results for COQ9, COQ8, and COQ7 are illustrated. Note that the mRNA level is highly up-regulated in response to cold exposure for the three genes (*$P < 0.01$, student's *t*-test). □: Control; ▨: Cold-adapted.

3 Discussion

Due to the quite opposite physiological functions of white and brown adipose tissues, comparative study of both tissues is important for elucidating the unique process of energy metabolism in BAT. Previous studies described an analysis of mitochondrial functions in white and brown adipocytes in mice[30]. In the study presented here, we examined mitochondrial proteomics in rat adipose tissues by using 2-DE analysis coupled with mass spectrometry, producing well-resolved protein spots, reliable quantification of protein level, and accurate protein identification. We learnt that the proteomics of BAT and WAT are substantially different qualitatively and quantitatively and are modulated by cold exposure, and the identified proteins can be classified into groups that function in lipid metabolism, amino acid metabolism, citrate acid cycle, oxidative phosphorylation, signaling, and protein synthesis. Our major findings are discussed in details below.

Both WAT and BAT are equipped with the necessary "machinery" for lipogenesis and lipolysis. In response to energy demands, the fatty acids can be mobilized from adipose stores for use by other tissues. When organism is at rest, all energy expenditure is equal to heat produced, which can occur in brown adipocytes by fatty acid oxidation. The β-oxidation of fatty acids occurs in mitochondrial matrix *via* four recurring steps, catalyzing by acyl-CoA dehydrogenase, enoyl-CoA hydratase, 3-HCDH and 3-ketoacyl-CoA thiolase. In our study, the expression levels of two of them were more abundant in BAT (spots *14*, *15*, *31*, *36*, *37*, *42*, and *43*) which were consistent with the results at mRNA levels[32]. In addition, our data showed the expression of ETF was up-regulated in BAT (spots *32*, *33*, *34*, *45*, and *46*). ETF accepts reducing equivalents from the acyl-CoA dehydrogenases, and then transfers the electrons to the respiratory chain, and the high expression of ETF agrees with a general increase of the β-oxidation flux in BAT. This demonstrates that the basal lipolytic activity is distinctly different between the two tissues, and the metabolism of fatty acids is overall increased in BAT.

BAT possesses a high activity of HMG-CoA lyase which plays an essential role in leucine catabolism[33]. Leucine oxidation in mitochondria gives rising to acetyl CoA and acetoacetyl CoA, and acetyl CoA enters into TCA cycle and yields NADH and $FADH_2$ that can be utilized for oxidation phosphorylation. In our study HMG-CoA lyase was up-regulated in BAT (spot 16). The expression further increased in brown fat mitochondria after cold exposure. We also found the expression of branched-chain keto-acid dehydrogenase (BCKD) (spot *24*) and isovaleryl

coenzyme A dehydrogenase (spot *26*) were increased. Both of them are involved in leucine catabolism, and BCKD complex is assumed to be the first rate-limiting step in mitochondrial leucine metabolism. These results suggest that the increasing of the leucine catabolism provides more substrate which can be utilized for energy production in BAT. Therefore, it is reasonable to assume that the mitochondrial leucine metabolism may be responsible for a supplementary pathway of providing energy in brown adipose tissue besides fat acid metabolism.

The up-regulation of pyruvate dehydrogenase E1 component(spots *20*, *21*, *22*, and *23*) and E2 component (spots *6* and *7*) suggests pyruvate availability is increased through an increase of glycolytic flux. This is likely to be connected with the increase of glucose uptake by brown adipocytes comparing with white adipocytes [34]. Thus, the citrate acid cycle substrate availability could be strongly increased. The expression of pyruvate dehydrogenase was increased, allowed acetyl-CoA to be over-produced from pyruvate in addition by high activity of β-oxidation and leucine metabolism. NAD^+-isocitrate dehydrogenase (IDH) is an important enzyme in the tricarboxylic acid cycle. It has been suggested that IDH is a rate-limiting enzyme in the oxidation of isocitrate, and the importance of NAD^+-IDH in energy metabolism in BAT has been evidenced by previous biochemical studies [35–36]. Previous studies have shown that the transcript levels of all three subunits of NAD^+-IDH in WAT are much lower than those in BAT [32], which were evidenced at the protein level in our study (spots *17*, *18*, and *19*). All these support the idea that there is a greater activity of the Krebs cycle in BAT than in WAT.

From a physiological point of view, the important difference between the two adipose tissues is the high respiratory, *i.e*. heat producing capacity of brown adipocytes compared to the very low respiratory capacity of white adipocytes. Our proteomic analysis showed that the expression levels of eight proteins involved in mitochondrial oxidative phosphorylation were increased in BAT. We identified 75 ku and 24 ku subunits of NADH dehydrogenase that were up-regulated (spots *1*, *2*, and *35*) in BAT, and the high activity of the complex Ⅰ in conjunction with the increased $FADH_2$ and NADH production through the Krebs cycle and β-oxidation would lead to an increase in the electron flux within the respiratory chain. Moreover, complexes Ⅲ and Ⅳ would also participate to this increased electron flux to the final acceptor, oxygen, as illustrated by high expression of ubiquinol-cytochrome c reductase and cytochrome c oxidase subunits. As a consequence of the high expression of complexes Ⅰ, Ⅲ and Ⅳ, the capacity of the respiratory chain electron transfer increases together with a raise of the proton pumping capacity. The increased electron flux within the respiratory chain due to high expression of respiratory enzymes explains the respiratory burst with thermogenic outcome of BAT. Thermogenesis in brown adipocytes is due to UCP-1 which is therefore classically considered to be the qualitative marker protein for BAT as compared to WAT[37]. In our study, UCP-1 was identified in BAT (spot *38*) but not found in WAT. These results are in perfect agreement with the results of Western blot (Figure 3). Interestingly, we found that F_1-ATPase β subunit was much down-regulated in BAT (spots *10* and *11*). The expression of ATPase is related to its physiological adaptations to demands of ATP. Mitochondria of BAT are naturally uncoupled from ATP synthesis which may lead to lower expression of ATPase. However, the mRNA levels for most ATPase subunits display an apparently high expression, which means that the expression of ATPase is regulated by post-transcriptional mechanisms. Previous studies have indicated that F_o-subunit c plays a key role in controlling the biosynthesis of F_1F_o-ATPase by affecting the complex assembly in BAT[38]. The exact reason for this discrepancy between the transcription and protein levels is still uncertain.

CoQ functions in mitochondrial respiratory electron transport, and is also known as an obligatory cofactor for H^+ transport by UCP-1[20], which argues for a physiological role of CoQ in the uncoupling of oxidative phosphorylation by UCP-1. In our study, COQ7, COQ8, and COQ9, which are required for CoQ biosynthesis and function in respiration, are highly up-regulated in BAT in response to cold exposure. Interestingly, COQ8 gene, required for Q biosynthesis, is demonstrated to be the same as the ABC1 gene in yeast[39]. ABC1 is assumed to function as a chaperone that is essential for the proper conformation and activity of abc1 and its neighboring complexes [40]. COQ8/ABC1 biochemical function in CoQ biosynthesis is currently unknown; however, high expression of the gene in BAT suggests that it may contribute to the unique process of energy metabolism in this tissue. To be noticed, the regulation of COQ gene expression upon cold exposure should be a complicated process.

To fully illustrate the mechanism, it will be necessary to detect more time points and extend the time span of the cold exposure for the mRNA and protein analysis in the future study.

In conclusion, we investigated the expression profiles of mitochondrial genes at the protein level in BAT and WAT and found that these proteins are involved in several processes and work cooperatively to establish a homeostasis adapting to the necessary of physiological function. The identification of differentially expressed proteins between WAT and BAT provides not only new insights into the mechanism of energy metabolism but also a good starting point for further dissection of their functions using other approaches. We have demonstrated that cold exposure induce activation of the defense mechanism in BAT. In this defense, COQ7, COQ8, and COQ9, which are considered to have both regulatory and kinetic roles in CoQ biosynthesis, are up-regulated and may play an important protective role in nonshivering thermogenesis in BAT.

References

[1] Cannon B, Nedergaard J. Brown adipose tissue: function and physiological significance. Physiol Rev, 2004, **84**(1): 277−359

[2] Nicholls D G, Locke R M. Thermogenic mechanisms in brown fat. Physiol Rev, 1984, **64**(1): 1−64

[3] Lidell M E, Enerback S. Brown adipose tissue-a new role in humans?. Nat Rev Endocrinol, 2010, **6**(6): 319−325

[4] Smith R E, Hock R J. Brown fat: thermogenic effector of arousal in hibernators. Science, 1963, **140**(3563): 199−200

[5] Puigserver P, Wu Z, Park C W, *et al*. A cold-inducible coactivator of nuclear receptors linked to adaptive thermogenesis. Cell, 1998, **92**(6): 829−839

[6] Bouillaud F, Ricquier D, Mory G, *et al*. Increased level of mRNA for the uncoupling protein in brown adipose tissue of rats during thermogenesis induced by cold exposure or norepinephrine infusion. J Biol Chem, 1984, **259**(18): 11583−11586

[7] Nedergaard J, Cannon B. The changed metabolic world with human brown adipose tissue: therapeutic visions. Cell Metab, 2010, **11**(4): 268−272

[8] Kozak L P. Brown fat and the myth of diet-induced thermogenesis. Cell Metab, 2010, **11**(4): 263−267

[9] Champigny O, Ricquier D. Effects of fasting and refeeding on the level of uncoupling protein mRNA in rat brown adipose tissue: evidence for diet-induced and cold-induced responses. J Nutr, 1990, **120**(12): 1730−1736

[10] Arch J R, Ainsworth A T, Cawthorne M A, *et al*. Atypical beta-adrenoceptor on brown adipocytes as target for anti-obesity drugs. Nature, 1984, **309**(5964): 163−165

[11] Rothwell N J, Stock M J. A role for brown adipose tissue in diet-induced thermogenesis. Nature, 1979, **281**(5726): 31−35

[12] Lowell B B, S-Susulic V, Hamann A, *et al*. Development of obesity in transgenic mice after genetic ablation of brown adipose tissue. Nature, 1993, **366**(6457): 740−742

[13] Wu Z, Puigserver P, Andersson U, *et al*. Mechanisms controlling mitochondrial biogenesis and respiration through the thermogenic coactivator PGC-1. Cell, 1999, **98**(1): 115−124

[14] Klingenberg M, Huang S G. Structure and function of the uncoupling protein from brown adipose tissue. Biochim Biophys Acta, 1999, **1415**(2): 271−296

[15] Brand M D, Brindle K M, Buckingham J A, *et al*. The significance and mechanism of mitochondrial proton conductance. Int J Obes Relat Metab Disord, 1999, **23**(Suppl 6): S4−11

[16] Ribeiro M O, Bianco S D, Kaneshige M, *et al*. Expression of uncoupling protein 1 in mouse brown adipose tissue is thyroid hormone receptor-beta isoform specific and required for adaptive thermogenesis. Endocrinology, 2010, **151**(1): 432−440

[17] Jia J J, Tian Y B, Cao Z H, *et al*. The polymorphisms of UCP1 genes associated with fat metabolism, obesity and diabetes. Mol Biol Rep, 2010, **37**(3): 1513−1522

[18] Enerback S, Jacobsson A, Simpson E M, *et al*. Mice lacking mitochondrial uncoupling protein are cold-sensitive but not obese. Nature, 1997, **387**(6628): 90−94

[19] Turunen M, Olsson J, Dallner G. Metabolism and function of coenzyme Q. Biochim Biophys Acta, 2004, **1660**(1−2): 171−199

[20] Echtay K S, Winkler E, Klingenberg M. Coenzyme Q is an obligatory cofactor for uncoupling protein function. Nature, 2000, **408**(6812): 609−613

[21] Rauchova H, Battino M, Fato R, *et al*. Coenzyme Q-pool function in glycerol-3-phosphate oxidation in hamster brown adipose tissue mitochondria. J Bioenerg Biomembr, 1992, **24**(2): 235−241

[22] Chaffee R R, Allen J R, Cassuto Y, *et al*. Biochemistry of brown fat and liver of Cold-acclimated hamsters. Am J Physiol, 1964, **207**(6): 1211−1214

[23] Kozak L P, Kozak U C, Clarke G T. Abnormal brown and white fat development in transgenic mice overexpressing glycerol 3-phosphate dehydrogenase. Genes Dev, 1991, **5**(124): 2256−2264

[24] Tran U C, Clarke C F. Endogenous synthesis of coenzyme Q in eukaryotes. Mitochondrion, 2007, **7**(Suppl): S62−71

[25] Meganathan R. Ubiquinone biosynthesis in microorganisms. FEMS Microbiol Lett, 2001, **203**(2): 131−139

[26] Asencio C, Rodriguez-Aguilera J C, Ruiz-Ferrer M, *et al*. Silencing of ubiquinone biosynthesis genes extends life span in *Caenorhabditis elegans*. Faseb J, 2003, **17**(9): 1135−1137

[27] Vajo Z, King L M, Jonassen T, *et al*. Conservation of the *Caenorhabditis elegans* timing gene clk-1 from yeast to human: a gene required for ubiquinone biosynthesis with potential implications for aging. Mamm Genome, 1999, **10**(10): 1000−1004

[28] Cannon B, Lindberg O. Mitochondria from brown adipose tissue: isolation and properties. Methods Enzymol, 1979, **55**(1): 65−78

[29] Yu X, Zhou Q, Li S C, *et al*. The silkworm (*Bombyx mori*) microRNAs and their expressions in multiple developmental stages.

PLoS One, 2008, **3**(8): e2997

[30] Forner F, Kumar C, Luber C A, *et al*. Proteome differences between brown and white fat mitochondria reveal specialized metabolic functions. Cell Metab, 2009, **10**(4): 324−335

[31] Navet R, Mathy G, Douette P, *et al*. Mitoproteome plasticity of rat brown adipocytes in response to cold acclimation. J Proteome Res, 2007, **6**(1): 25−33

[32] Unami A, Shinohara Y, Kajimoto K, *et al*. Comparison of gene expression profiles between white and brown adipose tissues of rat by microarray analysis. Biochem Pharmacol, 2004, **67**(3): 555−564

[33] Cooney G, Curi R, Mitchelson A, *et al*. Activities of some key enzymes of carbohydrate, ketone body, adenosine and glutamine metabolism in liver, and brown and white adipose tissues of the rat. Biochem Biophys Res Commun, 1986, **138**(2): 687−692

[34] Hernandez R, Teruel T, Lorenzo M. Akt mediates insulin induction of glucose uptake and up-regulation of GLUT4 gene expression in brown adipocytes. FEBS Lett, 2001, **494**(3): 225−231

[35] McCormack J G, Denton R M. Role of calcium ions in the regulation of intramitochondrial metabolism. Properties of the Ca^{2+}-sensitive dehydrogenases within intact uncoupled mitochondria from the white and brown adipose tissue of the rat. Biochem J, 1980, **190**(1): 95−105

[36] Shinohara Y, Daikoku T, Kajimoto K, *et al*. Expression of NAD(+)-dependent isocitrate dehydrogenase in brown adipose tissue. Biochem Biophys Res Commun, 2001, **281**(3): 634−638

[37] Klaus S, Casteilla L, Bouillaud F, *et al*. The uncoupling protein UCP: a membraneous mitochondrial ion carrier exclusively expressed in brown adipose tissue. Int J Biochem, 1991, **23** (9): 791−801

[38] Kramarova T V, Shabalina I G, Andersson U, *et al*. Mitochondrial ATP synthase levels in brown adipose tissue are governed by the c-Fo subunit P1 isoform. Faseb J, 2008, **22**(1): 55−63

[39] Hsieh E J, Dinoso J B, Clarke C F. A tRNA(TRP) gene mediates the suppression of cbs2-223 previously attributed to ABC1/COQ8. Biochem Biophys Res Commun, 2004, **317**(2): 648−653

[40] Bousquet I, Dujardin G, Slonimski P P. ABC1, a novel yeast nuclear gene has a dual function in mitochondria: it suppresses a cytochrome b mRNA translation defect and is essential for the electron transfer in the bc 1 complex. Embo J, 1991, **10**(8): 2023−2031

寒冷诱导产热时大鼠棕色脂肪能量代谢相关蛋白谱的变化

杨 悦[1, 2] 龚 未[1, 2] 王伟伟[1, 2] 俞晓敏[1] 胡松年[1] 于 军[1]*

([1] 中国科学院北京基因组研究所，基因组科学及信息重点实验室，北京 100029；[2] 中国科学院研究生院，北京 100049)

摘要 棕色脂肪组织(BAT)的生理作用与白色脂肪显著不同，它以产热的形式释放能量而不是将能量以 ATP 的形式储存．线粒体是在能量代谢和维持细胞稳态中具有重要功能的细胞器．为了更好地了解棕色脂肪中的能量代谢过程，运用双向电泳及质谱相结合的技术，分离了大鼠白色和棕色脂肪线粒体，对其差异蛋白质谱进行了系统分析和鉴定．参与脂肪和氨基酸代谢、三羧酸循环及线粒体呼吸链的蛋白质在棕色脂肪线粒体中的表达明显高于白色脂肪线粒体，在寒冷诱导下这些蛋白质的表达进一步上调．此外，参与辅酶 Q 合成的一系列 COQ 基因在棕色脂肪中经寒冷适应后表达明显上调．该研究表明，辅酶 Q 合成的增高在非颤栗性产热中具有重要作用，为进一步了解棕色脂肪特异性的能量代谢提供了新的思路．

关键词 棕色脂肪组织，寒冷适应，产热，辅酶 Q

学科分类号 Q256，Q413 **DOI**: 10.3724/SP.J.1206.2010.00231

* 通讯联系人.

Tel: 010-82995357, E-mail: junyu@big.ac.cn

收稿日期：2010-04-28，接受日期：2010-06-10